Journal of Biotechnology 168 (2013) 388–393

Contents lists available at ScienceDirect

Journal of Biotechnology

journal homepage: www.elsevier.com/locate/jbiotec

Fluorescein-labeled "arch-like" DNA probes for electrochemical detection of DNA on gold nanoparticle-modified gold electrodes

Lin Xu[a,1], Hao-ra Su[c,1], Gui-Rong Sun[a], Yan Wang[a], Shang-jing Guo[d], Xiao-ru Zhang[c], Shu-sheng Zhang[c], Shi-chao Xing[a,b,*]

[a] The Affiliated Hospital of Medical College Qingdao University, 266003, PR China
[b] Key Laboratory of Metabolic Diseases, Shandong Province, PR China
[c] Key Laboratory of Eco-chemical Engineering, Ministry of Education, College of Chemistry and Molecular Engineering, Qingdao University of Science and Technology, Qingdao 266042, PR China
[d] Pharmaceutical School of Liaocheng University, Liaocheng, PR China

ARTICLE INFO

Article history:
Received 24 April 2013
Received in revised form
26 September 2013
Accepted 30 September 2013
Available online 17 October 2013

Keywords:
E-DNA sensor
Gold nanoparticles
Electrodeposition
Fluorescein

ABSTRACT

In the present study, a gold nanoparticle-modified gold electrode (nanogold electrode) was used to develop a novel fluorescein electrochemical DNA biosensor based on a target-induced conformational change. The nanogold electrode was obtained by electrodepositing gold nanoparticles onto a bare gold electrode. This modification not only immobilized probe oligonucleotides, but also adsorbed fluorescein onto the surface of the gold nanoparticles to form an "arch-like" structure. This article compares the electrochemical signal changes caused by the hybridization of "arch-like" DNA on nanogold electrode and linear DNA on bare gold electrode. The results showed that the adsorption effect of nanogold can enhance the sensitivity of the sensor. The linear range of target ssDNA is from 2.0×10^{-9} M to 2.0×10^{-8} M with a correlation coefficient of 0.9956 and detection limit (3σ) of 7.10×10^{-10} M. Additionally, the specificity and hybridization response of this simple sensor were investigated.

1. Introduction

Recently, many electrochemical DNA (E-DNA) and similar electrochemical aptamer-based (E-AB) sensors have been developed based on the conformational changes of probe DNA dynamics (Liu et al., 2008; Lubin et al., 2006; Xiao et al., 2007; Zheng et al., 2013). Linear (Liu et al., 2008; Ricci et al., 2007a,b; Xiao et al., 2006) or stem-loop (Fan et al., 2003; Lai et al., 2006a,b; Lubin et al., 2006; Mao et al., 2003; Palecek, 2004; Ricci et al., 2007a,b; Xiao et al., 2007; Zheng et al., 2013) probe DNAs with a thiol at one end and a redox-active label at the other were self-organized onto a gold electrode with gold–thiol bonds. When bound to the target, the conformation of the probe DNA changed, significantly affecting the rate of electron transfer between the redox moiety and the electrode and producing a signal unique to the target. Such single-step, reagent-less electrochemical sensors have been widely used in detecting target DNA (Xiao et al., 2007), thrombin enzymes (Xiao et al., 2005), potassium ions (Radi and Sulliva, 2006), and small organic molecules (cocaine (Baker et al., 2006), adenosine triphosphate (Zuo et al., 2007), and theophylline (Ferapontova et al., 2008)). However, the conformations of some probe DNAs are very complicated, and further research is required to improve the sensitivity and binding ability of the simple sensors.

Gold nanoparticle assemblies have recently emerged as a promising class of materials for novel optical, electronic, catalytic, and sensing applications (Aldaye and Sleiman, 2007). Surface-enhanced Raman scattering studies showed (Krug et al., 1999; Nie and Emory, 1997) that fluorescent dyes could reversibly adsorb onto the surface of gold nanoparticles. Fluorescence measurements indicated (Maxwell et al., 2002) that the fluorophore at the distal end of an oligonucleotide molecule firmly tethered to a particle (via sulfur-metal bond) can loop back and adsorb the same particle to form a constrained "arch-like" structure. The fluorophore is then completely quenched by non-radiative energy transfer to the gold particle. This effect can be used in the field of electrochemistry for the detection of DNA. However, it remains to be investigated whether such constrained conformation can facilitate the hybridization process and enhance the electro signal change of an E-DNA sensor.

In the present paper, gold nanoparticles were directly electrodeposited onto bare gold electrode surfaces to form gold nanoparticle-modified electrodes. DNA probes labeled on opposite ends with thiol and fluorescein were then self-organized onto the

* Corresponding author at: The Affiliated Hospital of Qingdao Medical College, Qingdao University, Qingdao 266003, PR China. Tel.: +86 532 82912015; fax: +86 532 82911840.
E-mail address: ahmcqdu@gmail.com (S.-c. Xing).
[1] Both the authors Lin Xu and Hao-ra Su contributed equally.

0168-1656/$ – see front matter © 2013 Elsevier B.V. All rights reserved.
http://dx.doi.org/10.1016/j.jbiotec.2013.09.022

nanogold surface in a constrained conformation. Once hybridized with target DNA, the fluorescein dye was released, generating large changes in Faradaic current and allowing subsequent detection of target oligonucleotides.

2. Experiment

2.1. Materials and apparatus

2.1.1. Materials

Reagents were of analytical grade and used without further purification. Doubly distilled water was used throughout this work. $HAuCl_4$ was purchased from Tianjin Yingda Sparseness & Noble Reagent Chemical Factory. A 24-base, 3′thiol-, 5′fluorescein (F)-modified oligonucleotide (ssDNA-A) was obtained from Shanghai Huashun Biologic Engineering Company (Shanghai, China) and used as the probe DNA. The sequences of the probe DNA (ssDNA-A), target ssDNA complementary to the probe DNA (ssDNA-B), non-complementary ssDNA (ssDNA-C), and mis-complementary ssDNA (ssDNA-D, one-base mismatched to probe ssDNA-A) were as follows:

ssDNA-A: 5′-F-T_6-TAG GAA ACA CCA AAG ATG ATA TTT-T_6-SH-3′
ssDNA-B: 5′-AAA TAT CAT CTT TGG TGT TTC CTA-3′
ssDNA-C: 5′-TAC GAG TTG AGA GCA AGC AGA GTT-3′
ssDNA-D: 5′-AAA TAT CAT CTT TTG TGT TTC CTA-3′

2.1.2. Apparatus

All electrochemical measurements were performed on a CHI832B electrochemical analyzer (Shanghai, China). The voltammetry was carried out on a three-electrode system with a bare gold electrode as the working electrode, saturated calomel electrode (SCE) as the reference electrode, and Pt as the auxiliary electrode. Scanning electron microscopy (SEM) (JSM-6700F (JEOL, Japan)) was used to examine the morphology of the nanogold electrodes.

2.2. Gold nanoparticles deposition

The electrodeposition of gold nanoparticles on a bare gold electrode was carried out with a slight modification to the methods described by Liu et al. (2007) and Behzad et al. (2013). Briefly, the bare gold electrode (2 mm in diameter) was cleaned in a piranha solution (30% H_2O_2/70% H_2SO_4), rinsed with water, dried with nitrogen gas, and then cycled in a 0.1 M H_2SO_4 aqueous solution until a well-defined voltammogram was obtained. Gold nanoparticle electrodeposition was conducted by single potential mode in $HAuCl_4$ containing 0.1 M KNO_3 as the electrolyte. The electrode was then washed with deionized water to remove the nano-Au and characterized by SEM.

2.3. Immobilization and hybridization

Four microliter of 29 μM thiolated F-labeled probe DNA was evenly pipetted onto the surface of the freshly cleaned nanogold electrodes and left to air dry under ambient conditions over night. A small bottle was placed tightly over the electrode for gradual water evaporation. ssDNA probe immobilization was complete after rinsing with distilled water and drying with nitrogen gas. The ssDNA probe-modified electrodes were then immersed into PBS solution containing ssDNA-B, ssDNA-C or ssDNA-D at room temperature for 12 min. dsDNA-modified electrodes were also washed with distilled water and dried with nitrogen gas. The electrochemical responses caused by the electrochemical oxidation of fluorescein on ssDNA- or dsDNA-modified electrodes were determined using DPV in PBS (100 mM phosphate, 1.5 M NaCl, 1 mM Mg^{2+}, pH = 7.2).

3. Results and discussion

3.1. Characterization of nanogold-modified electrode surface

Fig. 1 shows the SEM images of the bare gold and nanogold electrode surfaces. The bare gold electrode (1a) was smooth with no visible gold particles while the nanogold electrode (1b) contained multiple layers of gold nanoparticles with interstices. Increasing deposition time yielded only a gradual increase in aggregate size (picture not shown).

3.2. Electro-signal change caused by DNA hybridization on the nanogold or bare gold electrodes

Good biocompatibility, large surface area, and strong electronic coupling have made gold nanoparticles important in the construction of DNA sensors (Lin et al., 2000). Although much effort has centered on increasing the amount of immobilized probe oligonucleotides, our experiments showed that a high amount of immobilized DNA, which can influence the hybridization efficiency, was not the only reason for signal changes caused by DNA

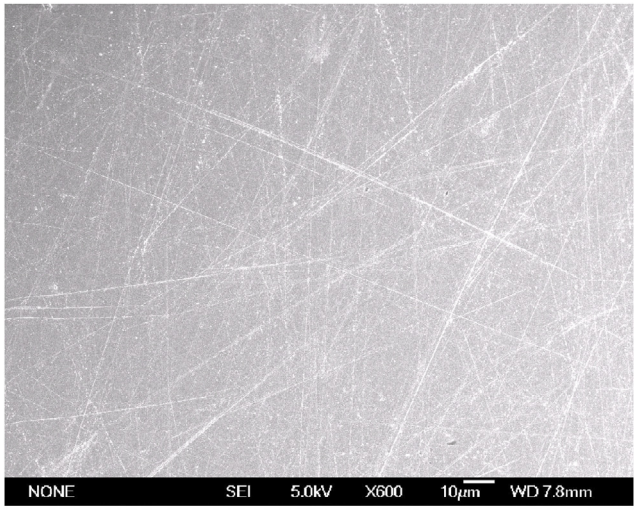

Fig. 1. SEM images of (a) the bare gold electrode; (b) the nanogold electrodes obtained by electrodepositing at the potential of −400 mV (vs. SCE) in 6 mM HAuCl4 for 300 s.

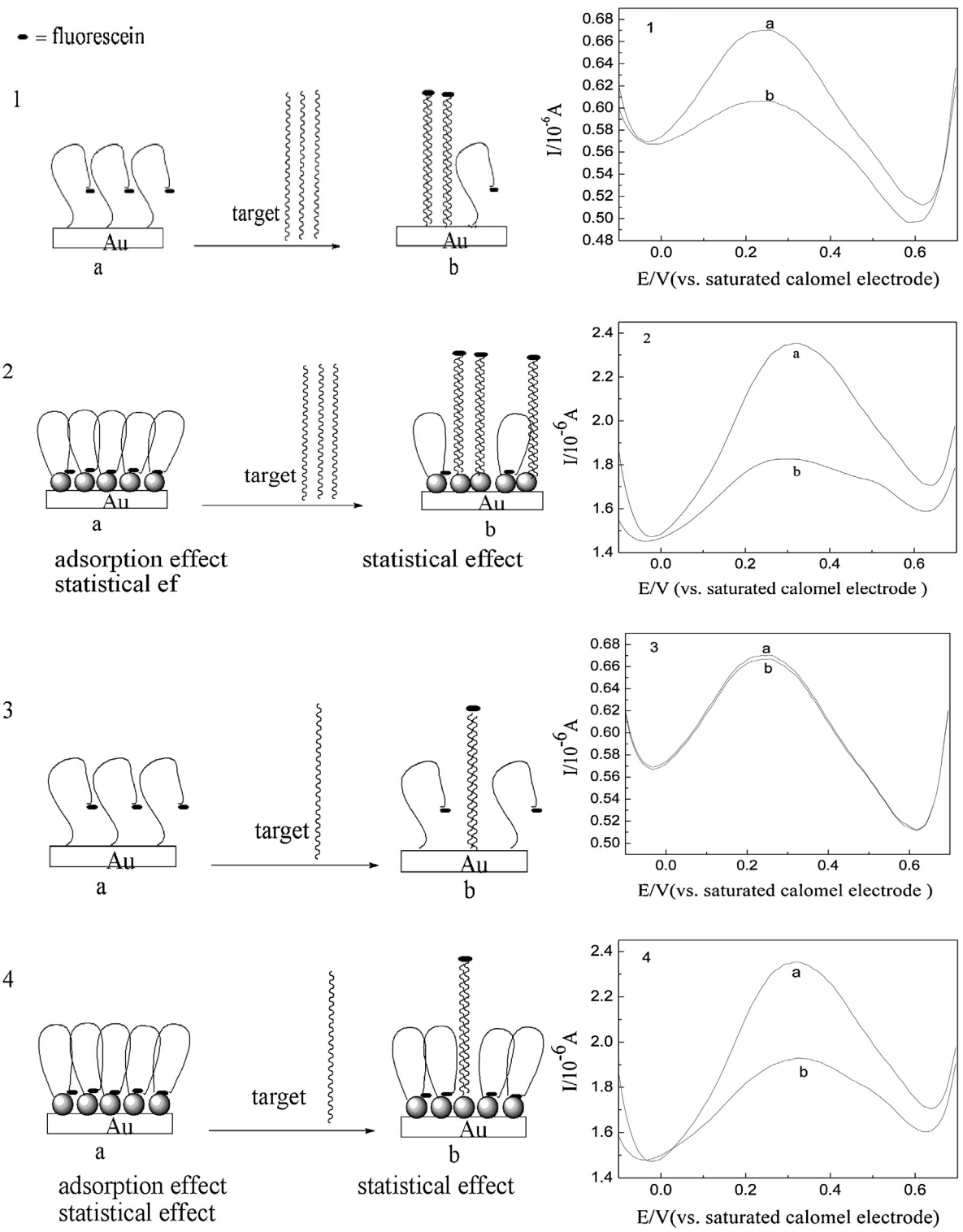

Fig. 2. DPV curves of bare gold electrode (1,3) and nanogold electrode (2,4): (a) probe DNA; (b) probe DNA plus 15 nM target DNA (1b,2b) or plus 5 nM target DNA (3b,4b).

hybridization on nanogold electrodes (Fig. 2). When the concentration of fully complementary target DNA was 15 nM, the observed signal suppression was about 43% on the bare gold electrode (Fig. 2(1)) and 77% on the nanogold electrode (Fig. 2(2)). Fluorescent dyes can reversibly adsorb onto the surface of gold nanoparticles (adsorption effect of nanogold) (Maxwell et al., 2002), which can further favor electron transfer. Thus, both the statistical and adsorption effects of nanogold can be attributed to the peak current enhancement on nanogold electrodes before hybridization (0.77 μA in Fig. 2(2-a)). However, only 0.13 μA signals on bare gold electrode were shown (Fig. 2(1-a)). After hybridization with target DNA, the "arch-like" structure opens to the extended rigid duplex form, which increases the distance between the fluorescein and electrode and reduces the Faradaic current. The adsorption effect of nanogold subsequently disappears, and the influence of nanogold to electro transfer can be ignored. Thus, we can conclude that the

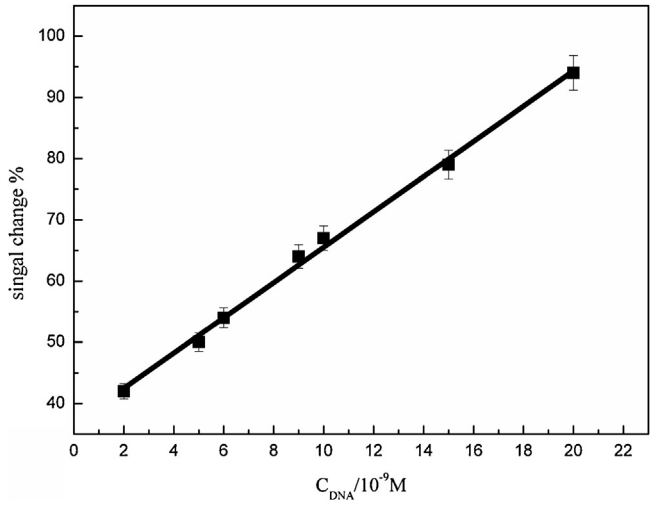

Fig. 3. The concentration of target ssDNA vs. the signal suppression percentage of peak current on nanogold electrodes. The error bars represent the standard deviation of four measurements conducted with a single electrode at each target DNA concentration.

adsorption effect of fluorescein to nanogold can contribute to the larger signal suppression on the nanogold electrode. When the concentration of fully complementary target DNA was as low as 5 nM, the changes of peak current after hybridization were almost undetectable on the bare gold electrode (Fig. 2(3)). However, the signal suppression of the nanogold electrode was still 50% (Fig. 2(4)). This shows that large conformational changes caused by the adsorption effect of nanogold can also give enough electrochemical signal changes even at low concentrations of target DNA.

To verify the above ideas, further experiments were carried out. First, ssDNA-A was immobilized on nanogold electrodes and bare gold electrodes. After hybridization with 15 nM of complementary target DNA, the number of hybridized ssDNA-B on the nanogold and bare gold electrodes was estimated from the UV–vis spectra (see Supplementary Materials, Fig. S7). The hybridization yield was 47% and 33% on the nanogold and bare electrodes, respectively. The DPV peak current change caused by single hybridization was 2.8×10^{-20} A on the nanogold electrode and 3.3×10^{-21} A on the bare electrode. From the results, we see that the high surface area of the nanogold electrode can enhance the hybridization efficiency. The larger DPV peak current change observed in the nanogold electrodes indicated that the conformation change caused by single hybridization on the nanogold electrode was similarly greater than that of the bare gold electrodes. This suggested that a difference existed in the conformation of the probe DNA immobilized on the nanogold and bare gold electrodes. Combined with the findings of Xiao et al. (2005), we believe that DNA with a thiol at one end and fluorescein at the other can adsorb onto nanogold electrodes and form an "arch-like" structure.

3.3. Detection limit for target DNA on optimal nanogold electrode

The sensitivity of the E-DNA sensor was investigated by varying the concentration of target ssDNA. The different signal intensities obtained after hybridization of the probe with target DNA were recorded from four different measurements. The peak current reflected the extent of hybridization between target ssDNA and excessive probe ssDNA. As shown in Fig. 3, the average decrease of the reductive peak was linear to the concentration of target ssDNA ranging from 2.0×10^{-9} M to 2.0×10^{-8} M. The regression equation was $y = 3.0641x + 35.897$ (x was the amount of the target DNA, 10^{-9} M; y was the signal suppression percentage), and the correlation coefficient was 0.9956. The detection limit for target ssDNA estimated using 3σ (where σ is the standard deviation of the blank solution, $n = 11$) was 7.10×10^{-10} M. Compared with other electrochemical DNA sensors shown in Table 1, the sensitivity of this sensor was moderate. However, the fabrication of this sensor was simpler without multiple amplification steps and, thus, is a more practical detection method.

Table 1
Comparison of electrochemical methods for DNA detection.

Assay	Detection limit of ssDNA	Ref.
Electroactive intercalator	1.94×10^{-8} M	Ding et al. (2008)
Au nanoparticles (cross-linked)	0.1 pM	Li et al. (2007)
Pb NPs amplification	0.3 pM	Zhu et al. (2004)
Silver NPs	0.5 pM	Cai et al. (2002)
Enzyme labels amplification	0.1 nM	Mao et al. (2008)
Au NPs	15 nM	Wang et al. (2001a)
Au NPs with Ag amplification	32 pM	Wang et al. (2001b)
Measurements based on the accumulation of purine nucleobases	0.8 nM	Wang and Kawde (2002)
Iposome amplification	50 fM	Patolsky et al. (2000)
Carbon-nanotubes loaded with CdS tags	6.6 pM	Wang et al. (2003)
E-DNA sensor based on the target-induced resolution of a DNA pseudoknot this method	2 nM 0.71 nM	Xiao et al. (2007)

3.4. The specificity between complementary and non-complementary DNA

On nanogold electrodes, the specificity of E-DNA sensors with "arch-like" structure is shown in Fig. 4. Unmodified nanogold electrodes showed no signal. When probe ssDNA-A was immobilized, a high peak current appeared. After hybridization at the same concentration, the current from a typical sensor was suppressed by 91% in the presence of perfectly complementary 24-base target (ssDNA-B), whereas the signal was suppressed by only 43% for 1-base mismatches (ssDNA-D) and <5% for non-complementary (ssDNA-C) DNA. The sequence specificities achieved on the nanogold electrode were similar to those measured by fluorescence, for which single-base mismatches resulted in a 55% signal decrease (Xiao et al., 2005), but higher than those of linear DNA probes (Ricci et al.,

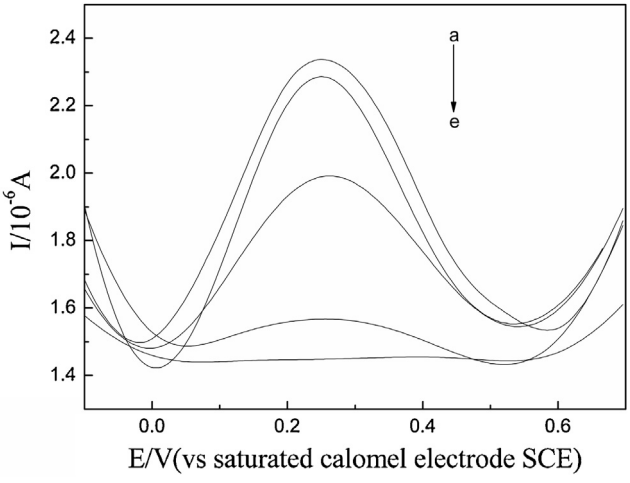

Fig. 4. (a) DPV curves of the probe ssDNA-A; (b) ssDNA-A plus 50 nM noncomplementary target ssDNA-C; (c) ssDNA-A plus 50 nM mis-complementary ssDNA-D; (d) ssDNA-A plus 50 nM perfectly complementary target ssDNA-B; (e) nanogold electrodes.

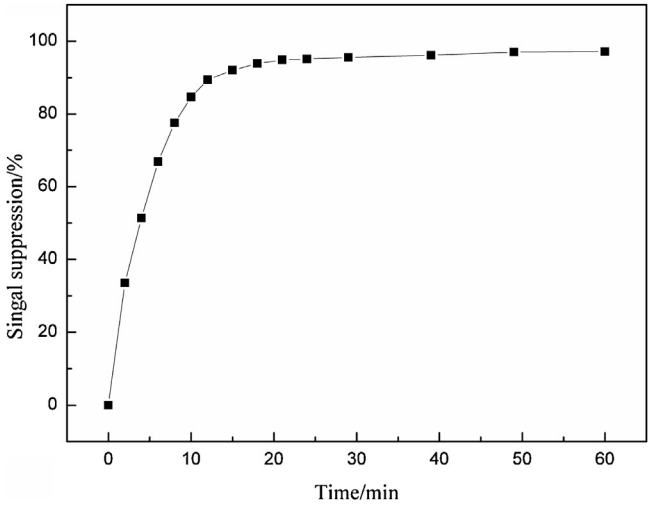

Fig. 5. Equilibration time of the E-DNA sensor: 90% of the saturating signal suppression was achieved after 12 min at 100 nM target concentration.

2007a,b) immobilized on bare gold electrodes, for which three-base mismatches resulted in about 80% signal decrease. These results coincide with previous studies, which revealed that conformationally constrained probes may offer higher hybridization specificities than linear probes (Bonnet et al., 1999). In this experiment, we used simple electrodeposition methods and line probe DNAs to form constrained "arch-like" structure that showed good specificity.

3.5. Effect of hybridization time

Fig. 5 illustrates the effect of hybridization time on DPV signal suppression. Hybridization times less than 12 min generated the greatest decrease in a linear plot. With longer hybridization times, the reduction in signal strength indicated the start of probe saturation. Compared with linear DNA probes (Ricci et al., 2007a,b) immobilized on bare gold electrode with sensor equilibration times between 2 and 30 min, our results showed that surface adsorption onto nanogold would not affect the response time. This may be attributed to the low surface adsorption energies of organic dyes on silver and gold (in the range of 8–16 kcal/mol), which are considerably smaller than the energies (ΔH = 80–100 kcal/mol) involved in DNA hybridization (Hildebrandt and Stockburger, 1984).

3.6. Reproducibility and regeneration

The reproducibility of the developed electrochemical biosensor was investigated using three nanogold-modified electrodes prepared in parallel. The relative standard deviation of the electrochemical response of the ssDNA probe was 7.1%, and was 7.6% for the ssDNA probe hybridized with target DNA. These results show that the developed electrochemical biosensor possessed good reproducibility.

The electrochemical DNA sensor is readily reusable. We successfully recovered up to 90% of the original signal by washing the electrode with water at 95 °C and re-challenging it with the target sequence. The minor signal loss arose during recovery may have been caused by the relative instability of fluorescein in aqueous solution at high temperatures.

4. Conclusions

In this work, DNA with thiol and fluorescein at opposing ends can adsorb onto nanogold electrodes and form an "arch-like" structure. Such direct contact adsorption can generate higher electro-transfer and lead to higher signal change after hybridization. Combined with high sensitivity and specificity, quick hybridization response, and ready re-usage, this simple method may be useful in making E-DNA and E-AB sensors for detecting DNA, enzyme, or small organic molecules. In addition, fluorescein, which has been widely used in optical sensors for its excellent optical character, is used as a redox label of E-DNA biosensors for the first time and shows good electrochemical redox signal. Whether other widely used redox-active labels such as methylene blue or ferrocene can adsorb onto the surface of colloidal silver and gold nanoparticles as fluorescent dyes still needs further investigation.

Conflict of interest

Authors claim to have no financial conflict of interest.

Acknowledgements

This work was supported by the National Natural Science Foundation of China (81100554), Shandong Provincial Natural Science Foundation, China (BS2012YY003), the Scientific and Technical Development Project of Department of health of Shandong Province (2011QZ007) and the Scientific and Technical Development Project of Qingdao (12-1-4-20-jch and 2012-1-3-2-(1)-nsh).

Appendix A. Supplementary data

Supplementary data associated with this article can be found, in the online version, at http://dx.doi.org/10.1016/j.jbiotec.2013.09.022.

References

Aldaye, F.A., Sleiman, H.F., 2007. Dynamic DNA templates for discrete gold nanoparticle assemblies: control of geometry, modularity, write/erase and structural switching. J. Am. Chem. Soc. 129, 4130–4131.

Baker, B.R., Lai, R.Y., Wood, M.S., Doctor, E.H., Heeger, A.J., Plaxco, K.W., 2006. An electronic, aptamer-based small-molecule sensor for the rapid, label-free detection of cocaine in adulterated samples and biological fluids. J. Am. Chem. Soc. 128, 3138–3139.

Behzad, M., Asgari, M., Shamsipur, M., Maragheh, M.G., 2013. Impedimetric and stripping voltammetric detection of sub-nanomolar amounts of mercury at a gold nanoparticle modified glassy carbon electrode. Biosens. Bioelectron. J. Electrochem. Soc. 160, B31–B36.

Bonnet, G., Tyagi, S., Libchaber, A., Kramer, F.R., 1999. Thermodynamic basis of the enhanced specificity of structured DNA probes. Proc. Natl. Acad. Sci. U. S. A. 96, 6171–6176.

Cai, H., Xu, Y., Zhu, N.N., He, P.G., Fang, Y.Z., 2002. An electrochemical DNA hybridization detection assay based on a silver nanoparticle label. Analyst 127, 803–808.

Ding, C., Zhao, F., Zhang, M.L., Zhang, S.S., 2008. Hybridization biosensor using 2,9-dimethyl-1,10-phenantroline cobalt as electrochemical indicator for detection of hepatitis B virus DNA. Bioelectrochemistry 72, 28–33.

Fan, C.H., Plaxco, K.W., Heeger, A., 2003. Electrochemical interrogation of conformational changes as a reagentless method for the sequence-specific detection of DNA. Proc. Natl. Acad. Sci. U. S. A. 100, 9134–9137.

Ferapontova, E.E., Olsen, E.M., Gothelf, K.V., 2008. An RNA aptamer-based electrochemical biosensor for detection of theophylline in serum. J. Am. Chem. Soc. 130, 4256–4258.

Hildebrandt, P., Stockburger, M., 1984. Surface-enhanced resonance Raman spectroscopy of Rhodamine 6G adsorbed on colloidal silver. J. Phys. Chem. C 88, 5844–5935.

Krug, J.T., Wang, J.D., Emory, S.R., Nie, S.M., 1999. Efficient Raman enhancement and intermittent light emission observed in single gold nanocrystals. J. Am. Chem. Soc. 121, 9208–9214.

Lai, R.Y., Lagally, E.T., Lee, S.H., Soh, H.T., Plaxco, K.W., Heeger, A.J., 2006a. Rapid, sequence-specific detection of unpurified PCR amplicons via a reusable, electrochemical sensor. J. Phys. Chem. C 103, 4017–4021.

Lai, R.Y., Seferos, D.S., Heeger, A.J., Bazan, G.C., Plaxco, K.W., 2006b. Comparison of the signaling and stability of electrochemical DNA sensors fabricated from 6- or 11-carbon self-assembled monolayers. Langmuir 22, 10796–10800.

Li, D., Yan, Y.M., Wieckowska, A., Willner, I., 2007. Amplified electrochemical detection of DNA through the aggregation of Au nanoparticles on electrodes and the incorporation of methylene blue into the DNA-crosslinked structure. Chem. Commun. 34, 3544–3546.

Lin, L., Zhao, H., Li, J., Tang, J., Duan, M., Jiang, L., 2000. Study on colloidal Au-enhanced DNA sensing by quartz crystal microbalance. Biochem. Biophys. Res. Commun. 274, 817–820.
Liu, G., Wan, Y., Gau, V., Zhang, J., Wang, L., Song, S., Fan, C., 2008. An enzyme-based E-DNA sensor for sequence-specific detection of femtomolar DNA targets. J. Am. Chem. Soc. 130, 6820–6825.
Liu, S.F., Wang, L., Zhao, F., 2007. Influence of gold nanoparticle modified electrode on the mediation reduction of ferricyanide by methylene blue. J. Electroanal. Chem. 602, 55–60.
Lubin, A.A., Lai, R.Y., Baker, B.R., Heeger, A.J., Plaxco, K.W., 2006. Sequence-specific, electronic detection of oligonucleotides in blood, soil, and foodstuffs with the reagentless reusable E-DNA sensor. Anal. Chem. 78, 5671–5677.
Mao, X., Jiang, J.H., Xu, X.M., Chu, X., Luo, Y., Shen, G.L., Yu, R.Q., 2008. Enzymatic amplification detection of DNA based on molecular beacon biosensors. Biosens. Bioelectron. 23, 1555–1561.
Mao, Y., Luo, C., Ouyang, Q., 2003. Studies of temperature-dependent electronic transduction on DNA hairpin loop sensor. Nucleic Acids Res. 31, e108.
Maxwell, D.J., Taylor, J.R., Nie, S., 2002. Self-assembled nanoparticle probes for recognition and detection of biomolecules. J. Am. Chem. Soc. 124, 9606–9612.
Nie, S., Emory, S.R., 1997. Probing single molecules and single nanoparticles by surface-enhanced Raman scattering. Science 275, 1102–1106.
Palecek, E., 2004. Surface-attached molecular beacons light the way for DNA sequencing. Trends Biotechnol. 22, 55–58.
Patolsky, F., Lichtenstein, A., Willner, I., 2000. Electrochemical transduction of liposome-amplified DNA sensing. Angew. Chem. Int. Ed. 39, 940–943.
Radi, A.E., Sulliva, C.K.O̓., 2006. Aptamer conformational switch as sensitive electrochemical biosensor for potassium ion recognition. Chem. Commun. 32, 3432–3434.
Ricci, F., Lai, R.Y., Heeger, A.J., Plaxco, K.W., Sumner, J.J., 2007a. Effect of molecular crowding on the response of an electrochemical DNA sensor. Langmuir 23, 6827–6834.
Ricci, F., Lai, R.Y., Plaxco, K.W., 2007b. Linear, redox modified DNA probes as electrochemical DNA sensors Electronic supplementary information (ESI) available: experimental procedures, controlling probe surface density, sensor equilibration time and specificity, the effect of target length and bulk on signaling, electron transfer rate measurements, and probe density effects on signaling. Chem. Commun. 36, 3768–3770.
Wang, J., Liu, G.D., Jan, M.R., Zhu, Q.Y., 2003. Electrochemical detection of DNA hybridization based on carbon-nanotubes loaded with CdS tags. Electrochem. Commun. 5, 1000–1004.
Wang, J., Polsky, R., Xu, D.K., 2001b. Silver-enhanced colloidal gold electrochemical stripping detection of DNA hybridization. Langmuir 17, 5739–5741.
Wang, J., Kawde, A.-N., 2002. Amplified label-free electrical detection of DNA hybridization. Analyst 127, 383–386.
Wang, J., Xu, D., Kawde, A.-N., Polsky, R., 2001a. Metal nanoparticle-based electrochemical stripping potentiometric detection of DNA hybridization. Anal. Chem. 73, 5576–5581.
Xiao, Y., Lubin, A.A., Baker, B.R., Plaxco, K.W., Heeger, A.J., 2006. Single-step electronic detection of femtomolar DNA by target-induced strand displacement in an electrode-bound duplex. Proc. Natl. Acad. Sci. U. S. A. 103, 16677–16680.
Xiao, Y., Piorek, B.D., Plaxco, K.W., Heeger, A.J., 2005. A reagentless signal-on architecture for electronic, aptamer-based sensors via target-induced strand displacement. J. Am. Chem. Soc., 17990–17991.
Xiao, Y., Qu, X., Plaxco, K.W., Heeger, A.J., 2007. Label-free electrochemical detection of DNA in blood serum via target-induced resolution of an electrode-bound DNA pseudoknot. J. Am. Chem. Soc. 129, 11896–11897.
Zheng, Y.J., Huang, Z.J., Chen, J., Wang, K., Liu, A.L., Lin, X.H., Zheng, W., 2013. Enzyme-based E-RNA sensor array with a hairpin probe: specific detection of gene mutation. Sensor Actuat. B-Chem. 181, 227–233.
Zhu, N.N., Zhang, A.P., Wang, Q.J., He, P.G., Fang, Y.Z., 2004. Lead sulfide nanoparticle as oligonucleotides labels for electrochemical stripping detection of DNA hybridization. Electroanalysis 16, 577–582.
Zuo, X., Song, S., Zhang, J., Pan, D., Wang, L., Fan, C., 2007. A target-responsive electrochemical aptamer switch (TREAS) for reagentless detection of nanomolar ATP. J. Am. Chem. Soc. 129, 1042–1043.